BRIEF ARTICLE

Diagnostic value for extrahepatic metastases of hepatocellular carcinoma in positron emission tomography/computed tomography scan

Ji Eun Lee, Jae Young Jang, Soung Won Jeong, Sae Hwan Lee, Sang Gyune Kim, Sang-Woo Cha, Young Seok Kim, Young Deok Cho, Hong Soo Kim, Boo Sung Kim, So Young Jin, Deuk Lin Choi

Ji Eun Lee, Jae Young Jang, Soung Won Jeong, Sang-Woo Cha, Young Deok Cho, Institution for Digestive Research, Digestive Disease Center, Department of Internal Medicine, Soonchunhyang University Hospital, Seoul 140-743, South Korea

Sae Hwan Lee, Hong Soo Kim, Institution for Digestive Research, Digestive Disease Center, Department of Internal Medicine, Soonchunhyang University Hospital, Cheon-an 330-721, South Korea

Sang Gyune Kim, Young Seok Kim, Boo Sung Kim, Institution for Digestive Research, Digestive Disease Center, Department of Internal Medicine, Soonchunhyang University Hospital, Bu-cheon 420-767, South Korea

So Young Jin, Department of Pathology, Soonchunhyang University Hospital, Seoul 140-743, South Korea

Deuk Lin Choi, Department of Radiology, Soonchunhyang University Hospital, Seoul 140-743, South Korea

Author contributions: Lee JE, Jang JY, Jeong SW and Choi DL wrote the paper; Lee SH, Kim SG, Cha SW, Kim YS, Cho YD, Kim HS, Kim BS and Jin SY provided clinical advice; Lee JE, Jang JY and Jeong SW performed the research.

Correspondence to: Dr. Jae Young Jang, Institute for Digestive Research, Digestive Disease Center, Department of Internal Medicine, Soonchunhyang University Hospital, 657, Hannam-dong, Yongsan-gu, Seoul 140-743, South Korea. jyjang@schmc.ac.kr

Telephone: +82-2-7099863   Fax: +82-2-7099797

Received: December 9, 2011 Revised: February 6, 2012

Accepted: February 16, 2012

Published online: June 21, 2012

Abstract

AIM: To evaluated the value of ^{18}F-fluorodeoxyglucose (FDG) positron emission tomography (PET)/computed tomography (CT) scan in diagnosis of hepatocellular carcinoma (HCC) and extrahepatic metastases.

METHODS: A total of 138 patients with HCC who had both conventional imaging modalities and ^{18}F-FDG PET/CT scan done between November 2006 and March 2011 were enrolled. Diagnostic value of each imaging modality for detection of extrahepatic metastases was evaluated. Clinical factors and tumor characteristics including PET imaging were analyzed as indicative factors for metastases by univariate and multivariate methods.

RESULTS: The accuracy of chest CT was significantly superior compared with the accuracy of PET imaging for detecting lung metastases. The detection rate of metastatic pulmonary nodule $\geq$ 1 cm was 12/13 (92.3%), when < 1 cm was 2/10 (20%) in PET imaging. The accuracy of PET imaging was significantly superior compared with the accuracy of bone scan for detecting bone metastases. In multivariate analysis, increased tumor size ($\geq$ 5 cm) ($P = 0.042$) and increased average standardized uptake value (SUV) uptake ($P = 0.028$) were predictive factors for extrahepatic metastases. Isometabolic HCC in PET imaging was inversely correlated in multivariate analysis ($P = 0.035$). According to the receiver operating characteristic curve, the optimal cutoff of average SUV to predict extrahepatic metastases was 3.4.

CONCLUSION: ^{18}F-FDG PET/CT scan is invaluable for detection of lung metastases larger than 1 cm and bone metastases. Primary HCC having larger than 5 cm and increased average SUV uptake more than 3.4 should be considered for extrahepatic metastases.

Hospital, 3-6-10 Otobashi Nakagawa-ku, Nagoya, Aichi 454-8509, Japan

INTRODUCTION

Most patients with hepatocellular carcinoma (HCC) present with underlying liver disease, usually cirrhosis, hepatitis B and hepatitis C virus infection[1,2]. Screening and surveillance programmes based on periodic ultrasonography and α-fetoprotein (AFP) among high-risk patients could establish of early diagnosis and provide more effective treatments of HCC[3]. With advances in variable treatment modalities, the prognosis of HCC has been much improved[4-7]. With prolonged survival of HCC patients, the incidence of extrahepatic metastases has been reported up to 42%[8]. Precise evaluation of extrahepatic metastases of HCC is important because treatment modality could be determined belong to the results.

Positron emission tomography (PET)/computed tomography (CT) scan using ^{18}F-fluorodeoxyglucose (FDG) is now well established as a noninvasive diagnostic tool for diagnosis, staging and monitoring of a variety of malignant tumors[9,10]. However, in detection of primary HCC, the sensitivity of ^{18}F-FDG PET/CT scan has been reported not sufficiently high (50%-55%) because of its variable ^{18}F-FDG uptake pattern[11-14].

Several studies were performed for investigation of usefulness of ^{18}F-FDG PET/CT scan in detection of extrahepatic metastases of HCC. A previous study reported that the sensitivity for the detection of extrahepatic metastasis was 79%[15,16]. However, there are few detailed reports to compare ^{18}F-FDG PET/CT scan with conventional imaging modalities.

In this study, we evaluated the value of ^{18}F-FDG PET/CT scan in diagnosis of primary HCC and extrahepatic metastases. Furthermore, we suggest several clinical factors and tumor characteristics including ^{18}F-FDG PET/CT scan findings that indicate extrahepatic metastases in diagnosis of HCC.

MATERIALS AND METHODS

Patients

We conducted a retrospective chart review of patients with HCC at Soonchunhyang University Hospital who had both conventional imaging modalities and ^{18}F-FDG PET/CT scan done within at least a month between November 2006 and March 2011. During this period, all patients diagnosed with HCC who were newly diagnosed or reevaluated after treatment underwent ^{18}F-FDG PET/CT scan. A total of 138 patients were enrolled for this study. Eighty-eight patients were treatment-naïve and the other 50 patients were previously treated for HCC (tumor resection, transcatheter arterial chemoembolization, radiofrequency ablation, systemic chemotherapy). The diagnosis of primary HCC was based on contrast enhanced abdomen CT or magnetic resonance imaging (MRI), where hyperattenuation in the arterial phase and early washout in the delayed phase were considered definitely diagnostic. Elevations in tumor markers such as AFP, protein induced by vitamin K antagonist Ⅱ (PIVKA Ⅱ) levels were considered suggestive of HCC. Ultrasound-guided needle biopsy was performed when considered necessary. This study was approved by the local institutional review board and was conducted in accordance with the principles set forth in the Declaration of Helsinki.

Conventional imaging modalities

Chest X-ray and contrast enhanced chest CT for evaluation of lung metastases were performed. If there are suspicious lesions, repeated contrast enhanced chest CT was examined within 3 mo. Whole body bone scan for evaluation of bone metastases was performed. If there are suspicious lesions, bone MRI was conducted for definite diagnosis or repeated bone scan was followed within 3 mo. Regional and distant lymph node metastases were determined according to contrast enhanced CT. If there are suspicious lesions, repeated contrast enhanced CT was examined within 3 mo to observe interval size difference. Some metastatic lesions were diagnosed with pathologic confirmation, but most metastatic lesions were clinically diagnosed because of difficult access to deep lesions and too small size to do a biopsy.

Intrahepatic tumor size was measured by the greatest diameter in treatment-naïve patients, and the greatest diameter including viable portion from the first diagnosis in previously treated patients.

^{18}F-FDG PET/CT scan

^{18}F-FDG PET/CT scan was performed with a Biograph 2 (Siemens Medical Solution, Knoxville, TN, United States). All patients fasted for at least 6 h before ^{18}F-FDG injection. Serum glucose levels measured at the time of ^{18}F-FDG injection were less than 150 mg/dL in all patients. Approximately 370-500 MBq of ^{18}F-FDG was injected intravenously and an emission scan (2.5 min/bed position) was performed from the knees to the head 40 min after of ^{18}F-FDG injection in the two dimensional imaging mode. A transmission scan (3 min/bed position) was then obtained with a rotating ^{68}Ge source.

^{18}F-FDG PET images were interpreted by one over 30 years experienced nuclear medicine physician. If no significant ^{18}F-FDG uptake was detectable in the tumor compared to normal liver tissue by ^{18}F-FDG PET/CT scan, this was considered isometabolic HCC, hypermetabolic HCC for increased ^{18}F-FDG uptake, and

Table 1 Patients baseline characteristics

	n = 138	%
Age	59.6 ± 11.1 (range: 33-84)	
Sex		
M/F	114/24	82.6/17.4
Etiology of liver disease		
HBV/HCV/alcohol/unknown	89/15/10/24	64.5/10.9/7.2/17.4
AFP (ng/mL)	9512.9 ± 23 026.4	
PIVKA Ⅱ (mAU/mL)	854.2 ± 871.7	
Tumor morphology		
Nodular/infiltrating	78/60	56.5/43.6
Tumor size (mm)	69.8 ± 45.2	
Tumor number		
1/≥ 2	52/86	37.7/62.3
PVTT		
Yes	54	39.1
Child-Pugh classification		
A/B/C	77/56/5	55.8/40.6/3.6
Tumor stage[1]		
Ⅰ/Ⅱ/Ⅲ/Ⅳa/Ⅳb	7/34/26/22/49	5.1/24.6/18.8/15.9/35.5
SUV		
Iso-/hypometabolism	42/3	30.4/2.2
Hypermetabolism	93	67.4
Maximum	5.32 ± 2.38	
Average	4.03 ± 1.26	
TNR (SUV ratio)	1.60 ± 0.49	
Extrahepatic metastases	50	36.2
Lung	23	46.0
Lymph nodes	22	44.0
Bone	11	22.0
Others[2]	5	10.0

[1]Tumor stage based on the Modified Union for International Cancer Control Tumor Node Metastasis staging system; [2]Others: Adrenal gland, peritoneal carcinomatosis, Morrison's pouch. HBV: Hepatitis B virus; HCV: Hepatitis C virus; AFP: α-fetoprotein; PIVKA Ⅱ: Protein induced by vitamin K antagonist Ⅱ; PVTT: Portal vein tumor thrombosis; SUV: Standardized uptake value; TNR: Tumor-to-nontumor ratio.

hypometabolic HCC for decreased ^{18}F-FDG uptake. Isometabolic or hypometabolic HCC was excluded from quantitative evaluation. For measurement of ^{18}F-FDG uptake, region of interest (ROI) was placed over tumor lesion including the area of maximum activity. The highest value of ^{18}F-FDG uptake in ROI is defined as maximum standardized uptake value (SUV) and the average value of ^{18}F-FDG uptake in ROI is defined as average SUV. Then, ROI was placed over nontumor area sized 20 mm × 20 mm for estimation of average ^{18}F-FDG uptake of nontumor area. SUV was calculated by as follows; mean tissue activity (kBq/mL) × calibration factor × body weight (kg)/injected dose (MBq). The tumor-to-nontumor ratio (TNR, SUV ratio) was calculated by average tumor SUV/average nontumor SUV.

Histologic examination

Histologic examination was performed to assess the histologic grade of HCC (*n* = 50). Twenty-nine patients were indicated for tumor resection at diagnosis, the other 21 patients were performed ultrasound-guided needle biopsy. According to histologic grade, the tumors were divided into low-grade (well-differentiated and moderately-differentiated type) and high-grade (poorly-differentiated

and undifferentiated type). As 4 patients were revealed as combined HCC-CC (cholangiocarcinoma), a total of 46 patients were analyzed.

Statistical analysis

Data are expressed as the mean ± SD, range, or *n* (%) as appropriate. When comparing the baseline characteristics of patients with 2 different groups, chi-square test and Fisher's exact test were used for categorical data, and the Student *t* test and *U* test were used for continuous variables. We performed receiver operating characteristic (ROC) curve analysis to compare the diagnostic performance of conventional and PET imaging for detection of extrahepatic metastasis. To estimate risk factors for extrahepatic metastases of HCC, univariate and subsequent multivariate logistic regression analysis were used. The overall cumulative survival rate was analyzed using the Kaplan-Meier method, and differences in survival between the groups were compared using a log-rank test. Data analysis was performed using SPSS 17.0 and MedCalc.

RESULTS

Patient characteristics

Patient characteristics are summarized in Table 1. Eighty-six patients (62.3%) had multiple lesions and 54 patients (39.1%) had portal vein thrombosis. Child-Pugh class A was 77 patients (55.8%), 56 patients (40.6%), and stage Ⅳb was 49 patients (35.5%) based on the modified Union for International Cancer Control Tumor Node Metastasis staging system.

Correlation between ^{18}F-FDG uptake and tumor differentiation

Forty-five of 138 patients (32.6%) with HCC did not have ^{18}F-FDG uptake. Therefore, SUV (maximum and average) was calculated in 93 patients (67.4%). The maximum SUV was 5.32 ± 2.38, average SUV was 4.03 ± 1.26, and tumor-to-nontumor ratio (TNR) was 1.60 ± 0.49 (Table 1). We analyzed the correlation of histologic grade in HCC with clinical factors and tumor characteristics including ^{18}F-FDG PET/CT scan findings (Table 2). Forty-six patients were performed tumor resection or ultrasound-guided needle biopsy and assessed the histologic grade.

In HCC with isometabolism, low-grade HCC was found in 14 patients and high-grade HCC in 2 patients; Isometabolic HCC tended to be histologically low-grade rather than high-grade ($P = 0.061$). In hypermetabolic HCC, maximum SUV value was higher in high-grade HCC than low-grade HCC ($5.75 ± 2.15$ *vs* $3.75 ± 0.74$, $P = 0.027$) although average SUV and TNR (SUV ratio) was not different between two groups (Table 2).

Diagnostic value of imaging modalities for detection of extrahepatic metastases

The results of the detection rate of conventional imaging modalities and ^{18}F-FDG PET/CT scan for extrahepatic metastases in HCC are summarized in Table 3.

Table 2 Correlation of histologic grade with clinical factors and tumor characteristics *n* (%)

	Low-grade (*n* = 34)	High-grade (*n* = 12)	*P* value[1]
Age	61.7 ± 8.4	56.5 ± 6.7	0.055
Sex			0.260
M/F	32 (94.1)/2	10 (83.3)/2	
Etiology of liver disease			0.431
HBV/HCV/alcohol/unknown	21/2/2/9	9/0/1/2	
AFP (ng/mL)	2892.0 ± 9255.6	2960.5 ± 9554.0	0.930
<200/≥ 200	26 (76.5)/8	10 (83.3)/2	
PIVKA II (mAU/mL) (*n* = 20/*n* = 7)	758.4 ± 823.1	798.6 ± 879.6	1.000
< 40/≥ 40	3 (15)/17	1 (16.7)/6	
Tumor morphology			0.441
Nodular/infiltrating	24 (70.6)/10	8 (66.7)/4	
Tumor size			0.643
< 5/≥ 5	16 (47.1)/18	7 (58.3)/5	
Tumor number			0.297
1/≥ 2	20 (58.8)/14	9 (75)/3	
PVTT			0.259
Yes	8 (23.5)	1 (8.3)	
Child-Pugh classification			0.563
A/B/C	30 (88.2)/4/0	11(91.7)/1/0	
T stage			0.537
1/2/3/4	3/15/9/7	1/7/2/2	
SUV			
Isometabolism	14 (41.2)	2 (16.7)	0.061
Hypometabolism	2	0	
Hypermetabolism (*n* = 18/*n* = 10)			
Maximum	3.75 ± 0.74	5.75 ± 2.15	0.027
Average	3.30 ± 0.42	4.15 ± 1.17	0.226
TNR (SUV ratio)	1.33 ± 0.22	1.64 ± 0.52	0.286

HBV: Hepatitis B virus; HCV: Hepatitis C virus; AFP: α-fetoprotein; PIVKA II: Protein induced by vitamin K antagonist II; PVTT: Portal vein tumor thrombosis; SUV: Standardized uptake value; TNR: Tumor-to-nontumor ratio. [1]Statistical significance test was done by *U* test.

Table 3 Diagnostic value of ^{18}F-fluorodeoxyglucose positron emission tomography/computed tomography scan and conventional imaging modalities for detection of extrahepatic metastases

	Lung metastases (*n* = 23)		Lymph node metastases (*n* = 22)		Bone metastases (*n* = 11)	
	TP	TN	TP	TN	TP	TN
PET (+)	14	1	20	4	11	0
Conventional (+)	23	2	22	4	7	4
	PET	Conventional	PET	Conventional	PET	Conventional
Sensitivity, %	60.9	100	90.9	100	100	63.6
Specificity, %	99.1	98.2	96.5	96.5	100	96.8
Accuracy, %	92.6	98.5	95.6	97.1	100	94.1
PPV, %	93.3	92	83.3	84.6	100	63.6
NPV, %	92.5	100	98.2	100	100	96.8
Comparison of ROC curves	*P* = 0.000 (CI: 0.0888-0.294)		*P* = 0.269		*P* = 0.010 (CI: 0.0481-0.348)	

TP: True positive; TN: True negative; PPV: Positive predictive value; NPV: Negative predictive value; ROC: Receiver operating characteristic; PET: Positron emission tomography.

Twenty-three patients were diagnosed of clinical lung metastases showing interval size increase on follow up chest CT. Fifteen patients were test positive on ^{18}F-FDG PET/CT scan, 14 patients were true positive and 1 patient turned out to be false positive revealing non-tuberculosis mycobacterium infection on percutaneous transthoracic needle aspiration (Figure 1). The detection rate of metastatic pulmonary nodule ≥ 1 cm was 12/13 (92.3%), when < 1 cm was 2/10 (20%) (*P* = 0.0003). The sensitivity, specificity, and accuracy for detection of lung metastases in HCC by ^{18}F-FDG PET/CT scan were 60.9%, 99.1% and 92.6%, respectively (Table 3). Contrast enhanced chest CT all detected for lung metastases in HCC and 2 lesions turned out to be false positive which did not show size increase during follow up chest CT. Therefore, the sensitivity, specificity and accuracy were 100%, 98.2% and 98.5%, respectively. The accuracy of chest CT was significantly superior compared with the accuracy of PET imaging for detecting lung metastases by comparison of ROC curves (*P* = 0.000, CI 0.0888-0.294) (Table 3).

Twenty-two patients were diagnosed of regional or distant lymph node metastases showing arterial phase enhancement and interval size increase on follow up contrast enhanced CT. The sensitivity of ^{18}F-FDG PET/CT scan for lymph node metastases was 90.9% showing lower than 100% in conventional imaging modalities. Both ^{18}F-FDG PET/CT scan and contrast enhanced CT detected 4 lesions as a positive test which turned out to be false positive. The accuracy of both images was not different by comparison of ROC curves (*P* = 0.269) (Table 3).

Eleven patients were diagnosed of bone metastases, ^{18}F-FDG PET/CT scan detected all of these lesions. However, bone scan failed to identify 4 patients and 4 suspicious of metastases turned out to be false positive. Therefore, the sensitivity, specificity and accuracy of ^{18}F-FDG PET/CT scan in diagnoses of bone metastases were 100%, 100% and 100%, respectively. The sensitivity, specificity and accuracy of bone scan were 63.6%, 96.8% and 94.1%, respectively. The accuracy of PET imaging was significantly superior compared with the accuracy of bone scan for detecting bone metastases by comparison of ROC curves (*P* = 0.010, CI: 0.0481-0.348) (Table 3).

Three patients with adrenal metastases were all detected by abdomen CT, but ^{18}F-FDG PET/CT scan failed to detect metastasis in one patient. There were 2 patients who were suspicious of cervical lymph node metastasis on both ^{18}F-FDG PET/CT scan and neck CT which turned out to be Warthin's tumor on needle biopsy.

### Indicative factors for extrahepatic metastases in ^{18}F-FDG PET/CT scan

Elevated AFP (≥ 200 ng/mL), elevated PIVKA II (≥ 40 mAU/mL), infiltrative tumor morphology, larger tumor size (≥ 5 cm), multiple tumors in liver, portal vein tumor thrombosis, advanced T stage, increased SUV uptake and high-grade HCC were associated with the presence of extrahepatic metastases of HCC (Table 4).

In multivariate analysis, increased tumor size (≥ 5 cm) (*P* = 0.042) and increased average SUV uptake (*P* = 0.028) were indicative factors for extrahepatic metastases in HCC (Table 4). Isometabolic HCC in ^{18}F-FDG PET/CT scan was inversely correlated with extrahepatic me-
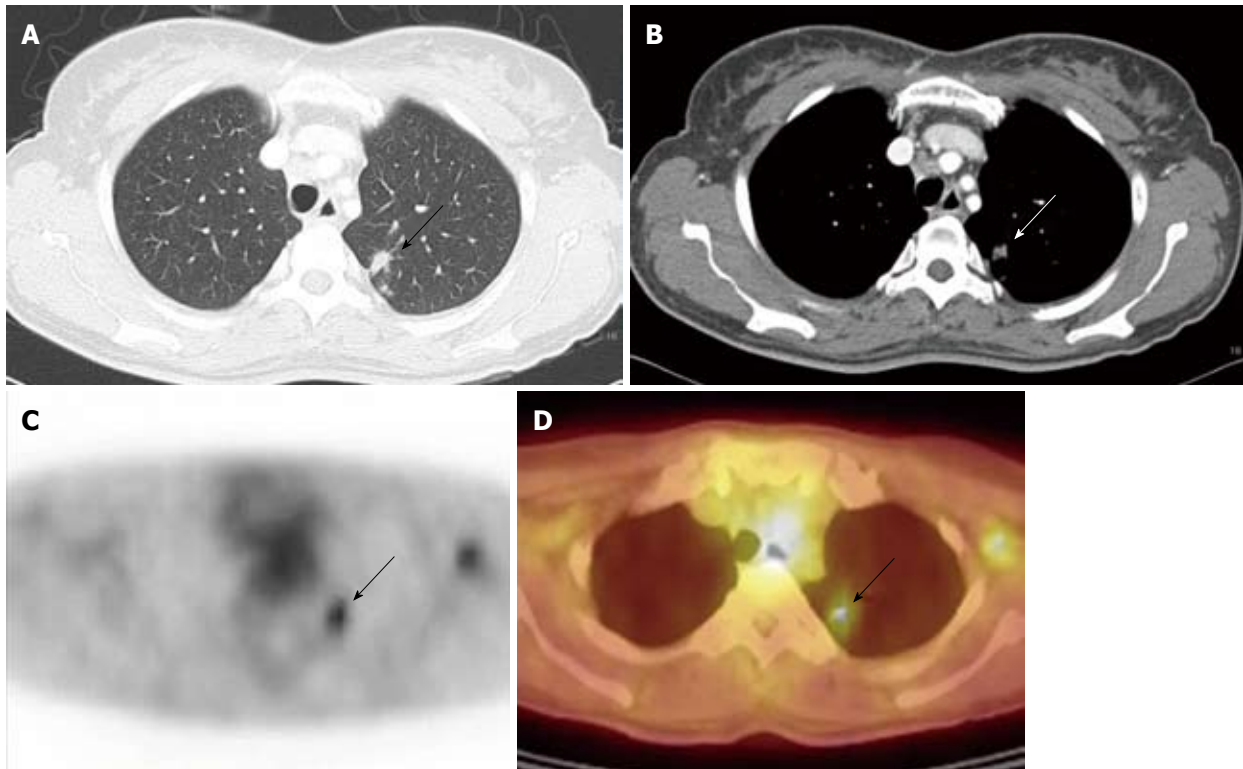
Figure 1 A 51 year-old-female with hepatocellular carcinoma was suspicious of lung metastasis (arrows) in both chest computed tomography and ^{18}F-fluorodeoxyglucose positron emission tomography/computed tomography scan which turned out to be nontuberculosis mycobacterium infection on percutaneous transthoracic needle aspiration. A: High-resolution computed tomography (CT); B: Contrast-enhanced CT; C: ^{18}F-fluorodeoxyglucose positron emission tomography (^{18}F-FDG PET); D: PET/CT scan.
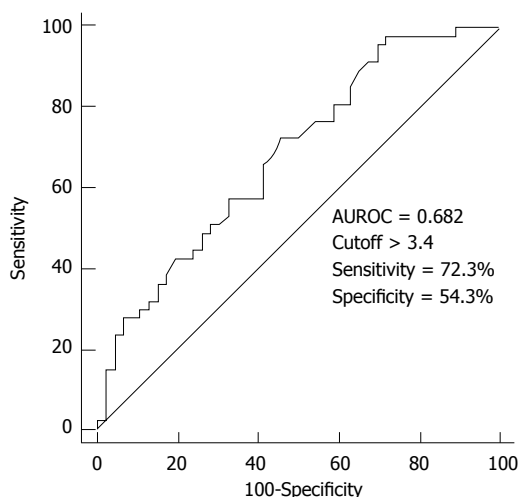
Figure 2 The area under the receiver operating characteristic curve to estimate the optimal cutoff of average standardized uptake value to predict extrahepatic metastasis. AUROC: Area under receiver operating characteristic.

tastases ($P = 0.035$). According to the ROC curve, the optimal cutoff of average SUV to predict extrahepatic metastases was > 3.4 (Figure 2). Therefore, when the average SUV in ROI is higher than 3.4, we should consider the possibility of extrahepatic metastases with poor prognosis.

Cumulative survival rate was studied by intrahepatic tumor size, average SUV, isometabolic HCC, and extra-

hepatic metastasis after dividing average SUV group into two groups by the cutoff 3.4. The survival rate was significantly higher in group with tumor size < 5 cm (1-year survival rate; 69.1% *vs* 25.9%, $P = 0.000$) (Figure 3A), average SUV < 3.4 (1-year survival rate; 57.1% *vs* 19.2%, $P = 0.000$) (Figure 3B), and isometabolic HCC (1-year survival rate; 78.0% *vs* 28.3%, $P = 0.000$) (Figure 3C). There were 2 clinical factors that affected survival rate of HCC by Cox proportional hazard analysis. Child-pugh class [class B: odds ratio (OR) 4.784, CI: 2.575-8.891, $P = 0.000$; class C: OR 10.787, CI: 3.579-32.511, $P = 0.000$] and metastases (OR 2.069, CI: 1.152-3.715, $P = 0.015$) were significantly associated with survival rate (Table 5).

DISCUSSION

Several investigators quantitatively evaluated glucose utilization in HCC with ^{18}F-FDG PET/CT scan and showed its usefulness for assessing characterization of tumor[17]. Increased tumor ^{18}F-FDG uptake is highly reflected the enzymatic activity of glucose metabolism and the histologic grading of HCC[17,18]. Well-differentiated HCC cells exhibit an ^{18}F-FDG metabolism similar to that of normal liver tissue, whereas undifferentiated HCC cells do not do so[17,19]. ^{18}F-FDG PET/CT scan was not sensitive than ultrasound and serum AFP levels for diagnosing HCC in HBV carriers[14]. Because of its limitations for intrahepatic lesions, ^{18}F-FDG PET/CT scan is not suitable as

Table 4 Clinical factors and tumor characteristics of extrahepatic metastases in hepatocellular carcinoma

	Metastasis (*n* = 50)	No metastasis (*n* = 88)	P value Uni	P value Multi
Age	58.7 ± 11.1	60.1 ± 11.1	0.480	
Sex			0.285	
M/F	39/11	75/13		
Etiology of liver disease			0.215	
HBV/HCV/alcohol/unknown	31/3/4/12	58/12/6/12		
AFP (ng/mL)	15 568.8 ± 28 119.6	6072.1 ± 18 882.3	0.019	0.254
< 200/≥ 200 (%)	21/29 (58.0)	59/29 (33.0)		
PIVKA II (mAU/mL)	1320.5 ± 784.0	630 ± 827.9	0.001	
< 40/≥ 40 (*n* = 25/*n* = 52) (%)	2/23 (92.0)	18/34 (65.4)		
Tumor morphology			0.000	0.126
Nodular/infiltrating (%)	17/33 (66.0)	61/27 (30.7)		
Tumor size	88.9 ± 40.2	58.9 ± 44.5	0.000	0.042[1]
< 5/≥ 5 (%)	7/43 (86.0)	48/40 (45.5)		
Tumor number			0.000	0.382
1/≥ 2 (%)	7/43 (86.0)	45/43 (48.9)		
PVTT			0.000	0.330
Yes (%)	30 (60.0)	24 (27.2)		
Child-Pugh classification			0.474	
A/B/C	35/11/4	68/19/1		
T stage			0.000	0.197
1/2/3/4 (%)	1/4/12/33 (66.0)	7/34/26/21 (23.9)		
SUV				
Isometabolism (%)	3 (6.0)	39 (44.3)	0.000	0.035
Hypometabolism	0	3		
Hypermetabolism (*n* = 47)				
Maximum	5.89 ± 2.55	4.74 ± 2.05	0.019	0.517
Average	4.38 ± 1.35	3.68 ± 1.05	0.006	0.028[2]
TNR (SUV ratio)	1.70 ± 0.51	1.50 ± 0.45	0.048	0.352
Pathology			0.042	
Low-/high-grade (*n* = 12/*n* = 34) (%)	7 (58.3)/5	27 (79.4)/7		

[1]1.06-31.8; [2]1.3-127.9. HBV: Hepatitis B virus; HCV: Hepatitis C virus; AFP: α-fetoprotein; PIVKA II: Protein induced by vitamin K antagonist II; PVTT: Portal vein tumor thrombosis; SUV: Standardized uptake value; TNR: Tumor-to-nontumor ratio.

Table 5 Clinical factors that affected survival by multivariate analysis

|	Odds ratio	CI	P value
Child class B	4.784	2.575-8.891	0.000
Child class C	10.787	3.579-32.511	0.000
AFP (> 200 ng/mL)	1.825	0.998-3.338	0.051
Tumor size (> 5 cm)	1.004	1.000-1.009	0.060
Metastases	2.069	1.152-3.715	0.015

a screening tool for detection of intrahepatic recurrence after tumor resection or liver transplantation[16].

In our study, 45 of 138 patients (32.6%) with HCC did not have ^{18}F-FDG uptake. Isometabolic HCC tended to be histologically low-grade (*P* = 0.061) and showed superior survival rate (*P* = 0.000). In this aspect, ^{18}F-FDG PET/CT scan might be useful for the prediction of outcome in patients with hepatocellular carcinoma. Yang *et al*[20] reported PET imaging could be a good preoperative tool for estimating the post-LT risk of tumor recurrence. It reported the overall survival rate was significantly lower in high SUV and high TNR group. Especially, TNR was independent predictor of survival in HCC patients in multivariate analysis[18,21]. The blood glucose level is often high in patients with cirrhosis[22],

affecting the SUV in the tumor region[23]. Therefore, TNR, tumor-to-nontumor SUV ratio more strongly correlated with characteristics of HCC than SUV[21]. In our study, the cumulative survival rate in the group with average SUV less than 3.4 was significantly higher than in the group with average SUV more than 3.4.

Extrahepatic metastases of HCC was occurred in 36.2% (29.5% in treatment-naïve patients) in our study which have been reported to occur in 13.5%-42%[24-27]. Major metastatic sites from HCC are the lung, lymph nodes, bone, and adrenal gland consistent with other reports[24-26,28].

It is known that lungs are both the most common site of metastases and the most common site of the first detectable metastases[16,24,25,28]. Chest X-ray is inexpensive, may serve as a baseline investigation to evaluate abnormalities, however, the detection rate of pulmonary metastases is low. Gielen *et al*[29] reported 10/19 patients with pulmonary metastases were not identified with chest X-ray in patients with colorectal cancer. To compare chest CT with ^{18}F-FDG PET/CT scan, the accuracy of chest CT was higher than ^{18}F-FDG PET/CT scan in our study. The detection rate of ^{18}F-FDG PET/CT scan was only 20% when metastatic pulmonary nodule < 1 cm. Therefore, to detect early lung metastases from
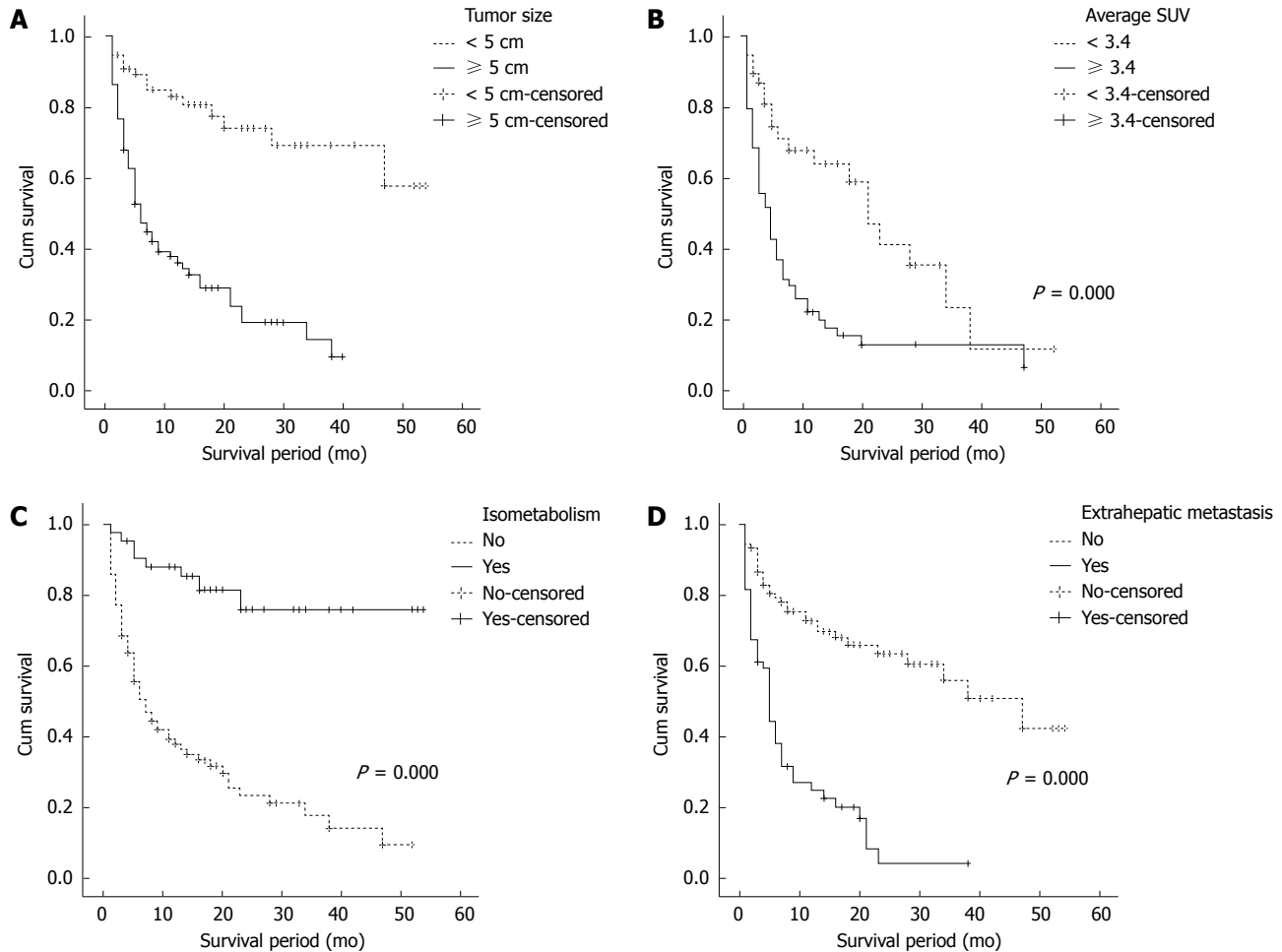
Figure 3 Cumulative survival rate in patients with hepatocellular carcinoma by intrahepatic tumor size (A), average standardized uptake value (B), isometabolic hepatocellular carcinoma (C) and extrahepatic metastasis (D). SUV: Standardized uptake value.

HCC, chest CT should be performed at regular intervals.

The diagnosis of regional or distant lymph node metastases is determined by interval size increase and arterial phase enhancement in abdomen CT/MRI, chest CT and neck CT[25]. It is well documented that patients who have cirrhosis also have benign enlarged lymph nodes[30]. In our study, 4 patients were detected for lymph node metastases, which turned out to be false positive in both ^{18}F-FDG PET/CT scan and contrast enhanced CT. Therefore, follow up CT is critical for determination of metastases even when increased ^{18}F-FDG uptake in ^{18}F-FDG PET/CT scan is observed. Lymph node metastasis is difficult to confirm due to poor accessibility for biopsy. If suspicious lesions were identified at conventional imaging or ^{18}F-FDG PET/CT scan, it should be clinically confirmed during follow-up imaging.

In our study, all bone metastases of HCC were detected by ^{18}F-FDG PET/CT scan whereas bone scan could not detect 4 lesions and 4 abnormal uptakes were false positive based on bone MRI and follow up imaging. Other studies have also reported PET imaging is more sensitive than bone scan[15,16,27]. Whole body bone scan is a routine modality in detecting bone metastases; however, lesions may remain invisible in the absence of an osteo-

blastic response. Furthermore, bone scan is not likely to differentiate healing fractures and degenerative disease from bone metastases[31]. Based on these results, ^{18}F-FDG PET/CT scan is more sensitive and specific diagnostic tool than bone scan for evaluation of bone metastases.

Although extrahepatic metastases of HCC are common, undergoing ^{18}F-FDG PET/CT scan in all HCC patients may not be cost-effective. Selected patients who are suspected of extrahepatic metastases of HCC should be performed of ^{18}F-FDG PET/CT scan. A previous study reported majority of patients (87%) with extrahepatic HCC had intrahepatic stage Ⅲ (10%) and stage Ⅳa (76%) tumors[25]. Natsuizaka *et al*[24] and Uka *et al*[26] also reported patients with more advanced intrahepatic tumor stage at the first diagnosis of HCC developed extraheaptic metastases more frequently. Especially, tumor diameter is a well-known predictor of extrahepatic metastases[27,28]. Our results demonstrated tumor size (≥ 5 cm) (P = 0.042) was predictive factors for extrahepatic metastases in HCC which was strongly correlated with cumulative survival rate.

As previously mentioned, the most common site of the first detectable metastasis is lung. Our data showed that the sensitivity of ^{18}F-FDG PET/CT scan to detect

lung metastases was only 60.9%. Therefore, we suggest that patients with diagnosed of HCC should undergo chest CT at initial diagnosis of HCC. Sixteen of 22 patients (72.7%) with lymph node metastases and 6 of 11 patients (54.5%) with bone metastases were not accompanied by lung metastases, so the patients at high risk of extrahepatic metastases or who was diagnosed of lung metastases by chest CT should be considered performing ^{18}F-FDG PET/CT scan to identify other extrahepatic metastases.

Our data showed that average SUV in ^{18}F-FDG PET/CT scan is indicative factor for extrahepatic metastases, staging evaluation for metastases should be done carefully at regular interval in patients with high average SUV uptake. The SUV is well correlated with histologic differentiation and cumulative survival rate, therefore we can apply this information in clinical settings to make a decision for the treatment and predict the prognosis. PET imaging is highly sensitive for the diagnosis of bone metastases, it should be considered to be done when patients are suspicious of bone metastases, but negative results in bone scan.

There were limitations to our study. (1) It was a retrospective study; (2) We did not confirm the extrahepatic metastases by biopsy; and (3) In histologic grading of intrahepatic HCC, needle biopsy is prone to sampling error as only limited area of the tumor is analyzed microscopically.

In conclusion, ^{18}F-FDG PET/CT scan has a limitation for detection of intrahepatic tumor, but meaningful for prediction of prognosis and planning for staging evaluation. In aspect of a screening tool of extrahepatic metastasis of HCC, ^{18}F-FDG PET/CT scan is invaluable for detection of lung metastases larger than 1 cm and bone metastases. In evaluation of lymph node metastases, follow-up imaging is crucial for clinical diagnosis. We suggest that primary HCC having larger than 5 cm and increased average SUV uptake more than 3.4 should be considered for extrahepatic metastases.

COMMENTS

Background
With advances in variable treatment modalities, the prognosis of hepatocellular carcinoma (HCC) has been much improved. With prolonged survival of HCC patients, the incidence of extrahepatic metastases has been increased.

Research frontiers
Positron emission tomography (PET)/computed tomography (CT) scan using fluorodeoxyglucose (FDG) is now well established as a noninvasive diagnostic tool for diagnosis, staging and monitoring of a variety of malignant tumors. However, the role in diagnosis of primary HCC and extrahepatic metastases has not been reported sufficiently.

Innovations and breakthroughs
^{18}F-FDG PET/CT scan has a limitation for detection of intrahepatic tumor, but meaningful for prediction of prognosis and planning for staging evaluation. The detection rate of metastatic pulmonary nodule $\geq$ 1 cm was 12/13 (92.3%), when < 1 cm was 2/10 (20%) in PET imaging. The accuracy of PET imaging was significantly superior compared with the accuracy of bone scan for detecting bone metastases. In multivariate analysis, increased tumor size ($\geq$ 5 cm) (P = 0.042) and increased average standardized uptake value (SUV) uptake (P = 0.028) were predictive factors for extrahepatic metastases.

Applications
The study results suggest that ^{18}F-FDG PET/CT scan is invaluable for detection of lung metastases larger than 1 cm and bone metastases. Authors suggest that primary HCC having larger than 5 cm and increased average SUV uptake more than 3.4 should be considered for extrahepatic metastases.

Terminology
PET/CT scan: PET/CT scan depicts the spatial distribution of metabolic or biochemical activity in the body. PET/CT scan has revolutionized many fields of medical diagnosis, by adding precision of anatomic localization to functional imaging.

Peer review
This is a well-organized study in which authors analyze the substantial role in the diagnosis of extrahepatic metastases in HCC. Furthermore, the results are interesting that average SUV could suggest the prognosis of HCC. In patients with higher average SUV more than 3.4 should be carefully follow-up for the possibility of extrahepatic metastases.

REFERENCES

1   **Parkin DM**. The global health burden of infection-associated cancers in the year 2002. *Int J Cancer* 2006; **118**: 3030-3044

2   **Simonetti RG**, Cammà C, Fiorello F, Politi F, D'Amico G, Pagliaro L. Hepatocellular carcinoma. A worldwide problem and the major risk factors. *Dig Dis Sci* 1991; **36**: 962-972

3   **Trevisani F**, De NS, Rapaccini G, Farinati F, Benvegnù L, Zoli M, Grazi GL, Del PP, Di N, Bernardi M. Semiannual and annual surveillance of cirrhotic patients for hepatocellular carcinoma: effects on cancer stage and patient survival (Italian experience). *Am J Gastroenterol* 2002; **97**: 734-744

4   **Mazzaferro V**, Regalia E, Doci R, Andreola S, Pulvirenti A, Bozzetti F, Montalto F, Ammatuna M, Morabito A, Gennari L. Liver transplantation for the treatment of small hepatocellular carcinomas in patients with cirrhosis. *N Engl J Med* 1996; **334**: 693-699

5   **Arii S**, Yamaoka Y, Futagawa S, Inoue K, Kobayashi K, Kojiro M, Makuuchi M, Nakamura Y, Okita K, Yamada R. Results of surgical and nonsurgical treatment for small-sized hepatocellular carcinomas: a retrospective and nationwide survey in Japan. The Liver Cancer Study Group of Japan. *Hepatology* 2000; **32**: 1224-1229

6   **Lo CM**, Ngan H, Tso WK, Liu CL, Lam CM, Poon RT, Fan ST, Wong J. Randomized controlled trial of transarterial lipiodol chemoembolization for unresectable hepatocellular carcinoma. *Hepatology* 2002; **35**: 1164-1171

7   **Shiina S**, Teratani T, Obi S, Sato S, Tateishi R, Fujishima T, Ishikawa T, Koike Y, Yoshida H, Kawabe T, Omata M. A randomized controlled trial of radiofrequency ablation with ethanol injection for small hepatocellular carcinoma. *Gastroenterology* 2005; **129**: 122-130

8   **Si MS**, Amersi F, Golish SR, Ortiz JA, Zaky J, Finklestein D, Busuttil RW, Imagawa DK. Prevalence of metastases in hepatocellular carcinoma: risk factors and impact on survival. *Am Surg* 2003; **69**: 879-885

9   **Böhm B**, Voth M, Geoghegan J, Hellfritzsch H, Petrovich A, Scheele J, Gottschild D. Impact of positron emission tomography on strategy in liver resection for primary and secondary liver tumors. *J Cancer Res Clin Oncol* 2004; **130**: 266-272

10   **Rigo P**, Paulus P, Kaschten BJ, Hustinx R, Bury T, Jerusalem G, Benoit T, Foidart-Willems J. Oncological applications of positron emission tomography with fluorine-18 fluorodeoxyglucose. *Eur J Nucl Med* 1996; **23**: 1641-1674

11   **Khan MA**, Combs CS, Brunt EM, Lowe VJ, Wolverson MK, Solomon H, Collins BT, Di Bisceglie AM. Positron emission tomography scanning in the evaluation of hepatocellular carcinoma. *J Hepatol* 2000; **32**: 792-797

12   **Delbeke D**, Martin WH, Sandler MP, Chapman WC, Wright JK, Pinson CW. Evaluation of benign vs malignant hepatic lesions with positron emission tomography. *Arch Surg* 1998; **133**: 510-515; discussion 510-515

13 **Trojan J**, Schroeder O, Raedle J, Baum RP, Herrmann G, Jacobi V, Zeuzem S. Fluorine-18 FDG positron emission tomography for imaging of hepatocellular carcinoma. *Am J Gastroenterol* 1999; **94**: 3314-3319

14 **Jeng LB**, Changlai SP, Shen YY, Lin CC, Tsai CH, Kao CH. Limited value of 18F-2-deoxyglucose positron emission tomography to detect hepatocellular carcinoma in hepatitis B virus carriers. *Hepatogastroenterology* 2003; **50**: 2154-2156

15 **Sugiyama M**, Sakahara H, Torizuka T, Kanno T, Nakamura F, Futatsubashi M, Nakamura S. 18F-FDG PET in the detection of extrahepatic metastases from hepatocellular carcinoma. *J Gastroenterol* 2004; **39**: 961-968

16 **Kim YK**, Lee KW, Cho SY, Han SS, Kim SH, Kim SK, Park SJ. Usefulness 18F-FDG positron emission tomography/computed tomography for detecting recurrence of hepatocellular carcinoma in posttransplant patients. *Liver Transpl* 2010; **16**: 767-772

17 **Torizuka T**, Tamaki N, Inokuma T, Magata Y, Sasayama S, Yonekura Y, Tanaka A, Yamaoka Y, Yamamoto K, Konishi J. In vivo assessment of glucose metabolism in hepatocellular carcinoma with FDG-PET. *J Nucl Med* 1995; **36**: 1811-1817

18 **Seo S**, Hatano E, Higashi T, Hara T, Tada M, Tamaki N, Iwaisako K, Ikai I, Uemoto S. Fluorine-18 fluorodeoxyglucose positron emission tomography predicts tumor differentiation, P-glycoprotein expression, and outcome after resection in hepatocellular carcinoma. *Clin Cancer Res* 2007; **13**: 427-433

19 **Okazumi S**, Isono K, Enomoto K, Kikuchi T, Ozaki M, Yamamoto H, Hayashi H, Asano T, Ryu M. Evaluation of liver tumors using fluorine-18-fluorodeoxyglucose PET: characterization of tumor and assessment of effect of treatment. *J Nucl Med* 1992; **33**: 333-339

20 **Yang SH**, Suh KS, Lee HW, Cho EH, Cho JY, Cho YB, Yi NJ, Lee KU. The role of (18)F-FDG-PET imaging for the selection of liver transplantation candidates among hepatocellular carcinoma patients. *Liver Transpl* 2006; **12**: 1655-1660

21 **Shiomi S**, Nishiguchi S, Ishizu H, Iwata Y, Sasaki N, Tamori A, Habu D, Takeda T, Kubo S, Ochi H. Usefulness of positron emission tomography with fluorine-18-fluorodeoxyglucose for predicting outcome in patients with hepatocellular carcinoma. *Am J Gastroenterol* 2001; **96**: 1877-1880

22 **Megyesi C**, Samols E, Marks V. Glucose tolerance and diabetes in chronic liver disease. *Lancet* 1967; **2**: 1051-1056

23 **Langen KJ**, Braun U, Rota Kops E, Herzog H, Kuwert T, Nebeling B, Feinendegen LE. The influence of plasma glucose levels on fluorine-18-fluorodeoxyglucose uptake in bronchial carcinomas. *J Nucl Med* 1993; **34**: 355-359

24 **Natsuizaka M**, Omura T, Akaike T, Kuwata Y, Yamazaki K, Sato T, Karino Y, Toyota J, Suga T, Asaka M. Clinical features of hepatocellular carcinoma with extrahepatic metastases. *J Gastroenterol Hepatol* 2005; **20**: 1781-1787

25 **Katyal S**, Oliver JH, Peterson MS, Ferris JV, Carr BS, Baron RL. Extrahepatic metastases of hepatocellular carcinoma. *Radiology* 2000; **216**: 698-703

26 **Uka K**, Aikata H, Takaki S, Shirakawa H, Jeong SC, Yamashina K, Hiramatsu A, Kodama H, Takahashi S, Chayama K. Clinical features and prognosis of patients with extrahepatic metastases from hepatocellular carcinoma. *World J Gastroenterol* 2007; **13**: 414-420

27 **Yoon KT**, Kim JK, Kim do Y, Ahn SH, Lee JD, Yun M, Rha SY, Chon CY, Han KH. Role of 18F-fluorodeoxyglucose positron emission tomography in detecting extrahepatic metastasis in pretreatment staging of hepatocellular carcinoma. *Oncology* 2007; **72** Suppl 1: 104-110

28 **Kanda M**, Tateishi R, Yoshida H, Sato T, Masuzaki R, Ohki T, Imamura J, Goto T, Yoshida H, Hamamura K, Obi S, Kanai F, Shiina S, Omata M. Extrahepatic metastasis of hepatocellular carcinoma: incidence and risk factors. *Liver Int* 2008; **28**: 1256-1263

29 **Gielen C**, Sanli I, Stroeken L, Botterweck A, Hulsewé K, Hoofwijk A. Staging chest radiography is not useful in patients with colorectal cancer. *Eur J Surg Oncol* 2009; **35**: 1174-1178

30 **Dodd GD**, Baron RL, Oliver JH, Federle MP, Baumgartel PB. Enlarged abdominal lymph nodes in end-stage cirrhosis: CT-histopathologic correlation in 507 patients. *Radiology* 1997; **203**: 127-130

31 **Schmidt GP**, Reiser MF, Baur-Melnyk A. Whole-body MRI for the staging and follow-up of patients with metastasis. *Eur J Radiol* 2009; **70**: 393-400

S- Editor Gou SX   **L- Editor** A   **E- Editor** Li JY